

Total Solar Irradiance Monitor for the FY-3B Satellite – Space Experiments and Primary Data Corrections

Hongrui Wang · Huiduan Li · Jin Qi · Wei Fang

Received: 5 June 2014 / Accepted: 10 November 2014 / Published online: 29 November 2014
© Springer Science+Business Media Dordrecht 2014

Abstract We present space experiments of the *Total Solar Irradiance Monitor* (TSIM) on the FY-3B satellite. The total solar irradiance (TSI) has been measured by TSIM/FY-3B continuously for nearly four years, with some short data gaps. Overlapping measurements of the TSI are provided by the TSIM, with three electrical substitution radiometers that are mounted with different alignment angles onto the leading face of the satellite. TSI measurements are normalized to a distance of 1 AU and zero velocity with respect to the Sun. The relative uncertainty in the TSI measurements is 910 parts per million. TSI values measured with TSIM/FY-3B are around 1365 W m^{-2} , slightly lower than VIRGO/SOHO and higher than TIM/SORCE values. Most of the time, it is found that short time-scale variations in TSI detected by TSIM/FY-3B agree with other space TSI instruments.

Keywords Instrumentation · Radiometers · Total solar irradiance

1. Introduction

The *Total Solar Irradiance Monitor* (TSIM) has been operated on the FY-3B satellite for nearly four years since 11 November 2010 (Yang *et al.*, 2012; Fang *et al.*, 2014). The goal of

H. Wang · W. Fang (✉)

Changchun Institute of Optics, Fine Mechanics and Physics, Chinese Academy of Sciences, Dong
Nanhu Road 3888, Changchun 130033, China
e-mail: tsim01@sina.com

H. Wang

e-mail: wanghongrui03@sina.com

H. Li

Department of Chemistry and Life Science, Chuxiong Normal University, Lu Cheng Nan Road 546,
Chuxiong 675000, China
e-mail: lhd08@cxtc.edu.cn

J. Qi

National Satellite Meteorological Center, China Meteorological Administration, No.46, Zhongguancun
Nandajie, Beijing 100081, China
e-mail: qijin@cma.gov.cn

the TSIM experiment is to detect variations in the total solar irradiance (TSI) and to provide TSI records for science investigations, such as solar-forcing mechanisms on Earth's climate (Frohlich 2012, 2013; Kopp and Lean, 2011). The hardware design of the TSIM on FY-3B is inherited from the TSIM on FY-3A (Fang *et al.*, 2014). The software and operations of the instrument have been revised from TSIM/FY-3B, according to the flight experience of TSIM/FY-3A, such as background measurements.

TSIM/FY-3A and TSIM/FY-3B observe the Sun by scanning. It is different from satellites pointed at the Sun such as VIRGO on SOHO (Frohlich *et al.* 1995, 1997a, 1997b), TIM on SORCE (Kopp and Lawrence, 2005; Kopp, Lawrence, and Rottman, 2005), PICARD (Meftah *et al.*, 2014), or from instruments of Sun-pointed systems such as SOVIM on the ISS (Mekaoui *et al.*, 2010). Scanning here indicates that the TSI is measured only when the Sun sweeps the TSIM field of view (FOV), given that the FY-3 satellites do not point toward the Sun accurately in orbit. Almost all payloads of FY-3B are instruments for observing Earth, so that the FY-3B satellite flies with a stable attitude pointing toward Earth (Yang *et al.*, 2012). The TSIM on the FY-3B satellite has no pointing system for active solar tracking.

TSIM/FY-3B was developed by the Changchun Institute of Optics, Fine Mechanics and Physics for China Meteorological Administration (CMA). The TSIM is called 'SIM' at CMA.

TSIM/FY-3B operates in passive-scanning manner, similar to ERB/Nimbus-7. The disadvantage of the scanning is that the offset angle between the optical axis of electrical substitution radiometers (ESRs) and the incoming sunlight varies, requiring complex corrections for solar pointing errors in the science data of the TSI. The solar pointing errors of TSIM/FY-3B can be computed using ephemeris data and satellite orbit information, but their precise estimation is complicated and time-consuming. However, the scanning option of the TSIM has led to the flight opportunities provided by the FY-3B satellite.

2. Corrections for TSI

Raw TSI data produced by the TSIM are corrected for Sun–Earth distance, background thermal emission, and the offset angle of the incoming sunlight. Solar irradiance measurements of each absolute radiometer are normalized to a distance of 1 AU and zero velocity with respect to the Sun. The equation for deriving the value of TSI with corrections is

$$T_c = (E - E_b) f_{1 \text{ AU}} f_{\text{pointing}} f_{\text{Doppler}} f_c, \quad (1)$$

where T_c is the normalized TSI at 1 AU and zero velocity, E is the original irradiance measured with each ESR in TSIM, E_b is the irradiance of the thermal background measured in space, $f_{1 \text{ AU}}$ is a factor for Sun–Earth distance correction, f_{pointing} is a correction factor for the solar pointing error, f_{Doppler} is a factor for Doppler correction, and f_c is a correction factor for traceability (Kopp, Heuerman, and Lawrence, 2005; Fehlmann *et al.*, 2012; Kopp *et al.*, 2012).

The Sun–Earth distance $r_{\text{Sun–Earth}}$ is calculated by using the VSOP 87 theory (Bretagnon and Franco, 1988). In this theory, the motion of the planets is given in an analytical solution using elliptic elements, and the positions of the planets are derived using Poisson series expansion, based on different sets of coordinate representations. The Sun–Earth radius vector is given in heliocentric spherical coordinate variables. The reference frame for the Sun–Earth radius vector is the mean equinox and ecliptic of date.

Table 1 Uncertainties in TSIM/FY-3B measurements.

Parameter	Value	Relative uncertainty	Absolute uncertainty
E (original irradiance)	1302.841 W m ⁻²	510 ppm	0.664 W m ⁻²
E_b (thermal background irradiance)	-20.571 W m ⁻²	1354 ppm	0.281 W m ⁻²
$f_{1 \text{ AU}}$ (correction factor for the Sun–Earth distance)	1.029425374	200 ppm	2.058×10^{-4}
f_{pointing} (correction factor for the solar pointing error)	1.005678535	700 ppm	7.039×10^{-4}
f_c (correction factor for traceability)	0.996734948	100 ppm	9.967×10^{-5}
T_c (normalized TSI)	1365.621 W m ⁻²	910 ppm	1.243 W m ⁻²

Factor $f_{1 \text{ AU}}$ is given as

$$f_{1 \text{ AU}} = \left(\frac{r_{\text{AU}}}{r_{\text{Sun–Earth}}} \right)^2, \quad (2)$$

where r_{AU} is one astronomical unit. The correction factor for the solar pointing error is

$$f_{\text{pointing}} = \frac{1}{\cos \alpha}, \quad (3)$$

where α is the angle between the Sun and the optical axis of the radiometers. The solar pointing errors are described in detail in Section 3.

The factor for Doppler correction is

$$f_{\text{Doppler}} = \frac{c^2}{(c - v)^2}, \quad (4)$$

where c is the speed of light and v is the line-of-sight velocity of the satellite with respect to the Sun.

TSIM's traceability to the World Radiometric Reference (WRR) is achieved through ground-based comparison experiments in the air at ambient temperature and pressure (Wang, Li, and Fang, 2014). The list of uncertainties of TSIM/FY-3B in the space experiment is given in Table 1.

3. Solar Pointing Errors

The solar pointing error here denotes the offset angle between each radiometer's optical axis and the Sun vector. Solar pointing errors are generally determined with high accuracy by using a sun sensor. However, digital sun sensors were not employed to measure solar pointing errors of TSIM/FY-3B, owing to limitations in the budget and system resources. Therefore, we estimated the solar pointing errors based on astronomical computations. The Sun vector is first computed in the geocentric equatorial frame using astronomical ephemeris. Next, the Sun vector is transformed to the satellite frame through coordinate transformation. In this process the orbit data of the satellite are essential. The orbit data include the time of the observation and six orbital elements of the satellite (specific angular momentum, inclination, right ascension of the ascending node, eccentricity, argument of perigee, and true anomaly).

To achieve a better estimate of the solar pointing errors, the installation angles between the optical axis of three sets of ESRs (AR1, AR2, and AR3) and the x -axis of the FY-3B satellite are required to be precisely 22° , 27° , and 32° for AR1, AR2, and AR3, respectively. The installation angles between the optical axis of ESRs and the y -axis of the FY-3B satellite are expected to be precisely 68° , 63° , and 58° for AR1, AR2, and AR3, respectively. The optical axis of each ESR in the TSIM is required to be mounted accurately in the XOY plane of the satellite coordinate, strictly perpendicular to the z -axis of the satellite. The TSIM instrument was carefully mounted onto the leading surface of the satellite to satisfy these alignment requirements. The installation angles between the optical axis of each ESR and the x -axis or y -axis of the satellite were measured by theodolites and adjusted until they meet the requirements.

The solar pointing error of the radiometer AR1 is

$$\alpha_{\text{AR1}} = \alpha_{x-\text{AR1}} - \alpha_{sx}, \quad (5)$$

where $\alpha_{x-\text{AR1}}$ is the installation angle between the optical axis of AR1 and the x -axis of the satellite, and α_{sx} is the offset angle between the solar vector and the x -axis of the satellite. Similarly, we can define α_{AR2} and α_{AR3} .

4. Background Measurements

Each ESR installed in TSIM/FY-3B has a large FOV whose design value is 26.6° (Liebetaut *et al.*, 2013; Memarian and Eleftheriades, 2013; Witte *et al.*, 2014). The thermal background seen by each ESR cannot be neglected in the calibration to obtain TSI. When the satellite enters the Earth's shadow area, an ESR opens its shutter and thermal background is measured by each ESR for background compensation. It is assumed that the thermal state of the instrument in the Earth's shadow area (satellite night) is the same as the thermal state of the instrument in the sunlit area (satellite daytime). However, the temperature distribution in the instrument changes in the night and daytime of the satellite.

For TSIM/FY-3A, the thermal background was only measured when the telemetry commands were sent to the satellite from ground stations. For TSIM/FY-3B, the background measurements are made in an automatic manner, to avoid troublesome procedures of telemetry commands. The thermal background is measured once in each orbit automatically for all the three ESRs while in the Earth's shadow area.

5. ESR Operations in the Sunlit Time

As the solar vector seen by the radiometer changes with time, some of the radiometers in TSIM/FY-3B occasionally receive no sunlight because of their specific installation angles of the optical axis. Incoming sunlight with a large offset angle with respect to the optical axis of a radiometer is sometimes not strong enough for the radiometer to record real TSI values. Each radiometer has its own operation time and cannot measure TSI continuously in the orbit. Figure 1 shows the observing times of three ESRs and their TSI measurements.

When the incoming sunlight to a radiometer is too weak or when no sunlight is available, the radiometer stops its solar observing mode and the TSI is not measured. In such a stand-by mode without TSI measurement, the radiometer always keeps its shutter open to monitor the space, waiting for any incoming sunlight. The irradiance of the incoming light is regularly estimated for each ESR quickly with a simple scheme. If the irradiance estimated is higher

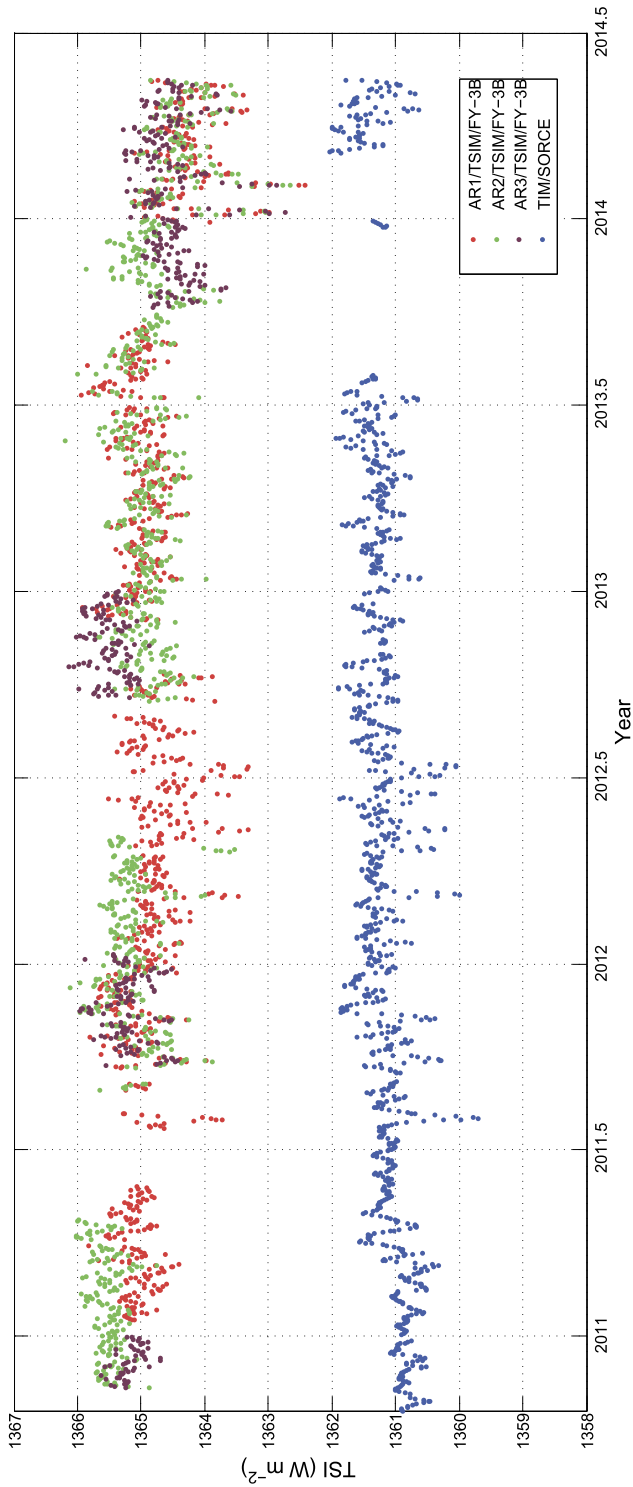


Figure 1 TSI measurements of TSIM/FY-3B (AR1, AR2, and AR3), in comparison with TIM/SORCE, from November 2010 to May 2014. Here 2013.5 in the abscissa approximately denotes 1 July 2013. All TSI data are daily averages.

than a pre-determined value, the incoming sunlight is considered to be strong enough to perform solar observations again and the ESR is enabled to work in the solar mode again.

Incoming sunlight is also influenced by the dynamics of the satellite in space. When the satellite changes its attitude in orbit, radiometer operations are inevitably impacted. An ESR expected to measure TSI may lose the opportunity of solar observations as a result of changes in the satellite attitude, such as the operation halt of AR1 from 28 September 2013 to 9 December 2013. Because of this, the expected overlapping measurements between AR1 in TSIM/FY-3B and TSIM/FY-3C were not made. TSIM/FY-3C, which measures TSI with a pointing system, started its daily TSI observations on 1 October 2013.

Some short data gaps of TSIM/FY-3B can be found in Figure 1, such as in September 2011 and July 2013. The short gaps are not attributed to changes in the solar vector, but to a failure of the analog-to-digital converter (ADC) in the TSIM. The ADC failure occurred several times in the experiment of TSIM/FY-3B. Heating voltages applied to the primary cavity and temperature difference between the heat sink and the primary cavity of each ESR are converted into digital signals by the ADC. The TSIM is not able to measure TSI during the ADC failure. The ADC failure is attributed to industrial (not space-qualified) chips used for the ADC in the instrument. The ADC chip was covered with a lead shield so that it could be used in space (Rubenchik, Fedoruk, and Turitsyn, 2014). However, its tolerance of space radiation was perhaps not adequate. It is a pity that a space-qualified ADC chip was not used in TSIM/FY-3B.

6. Comparisons with Other Space Experiments

TSIM/FY-3B has been operated continuously in orbit since 11 November 2010. A single TSI measurement or background measurement for each ESR lasts 11 min, which consists of a six-minute observation phase and a five-minute reference phase (Wang, Li, and Fang, 2014).

If the incoming sunlight is in the FOV of AR1 or AR2 and is strong enough, the TSI is observed once by AR1 or AR2 every orbit in the solar mode, as defined in the normal operation of TSIM/FY-3B. Radiometer AR3 has been designed for monitoring the degradation of the primary cavities of AR1 and AR2 (Anklin *et al.*, 1998; Frohlich 2003, 2009).

AR2 and AR3 were all enabled for daily observation for nearly 50 days, beginning on 11 November 2010, as shown in Figure 2. AR1 obtained first sunlight on 16 January 2011. The performance of AR3 in the initial 50 days was far from expectations. TSI measurements of AR3 had unexpected characteristics, and comparisons with AR2 or other space TSI instruments were not satisfactory. The incoming sunlight to AR3 was too weak to produce TSI measurements from 1 January 2011 to 31 January 2011. Furthermore, the Sun completely moved out of the AR3 FOV from February to September 2011, for nearly 210 days. The 210-day gap is much too long and was totally unexpected. Subsequently, no data were available for monitoring the degradation of the other two radiometers. AR3 was planned to be opened for one day for every 30 days for degradation monitoring.

In 2011, AR3 was not shut off to avoid complex telemetry commands from ground stations, but solar observing time of AR3 was quite short. Most of the time, it was in stand-by mode with its shutter open to detect any incoming sunlight. AR3 may receive sunlight in spring or summer. However, the offset angle between the incoming sunlight and the optical axis of AR3 was generally too large and too little energy was absorbed by its primary cavity to perform solar observations. As a result, the degradation of each ESR was not monitored for TSIM/FY-3B.

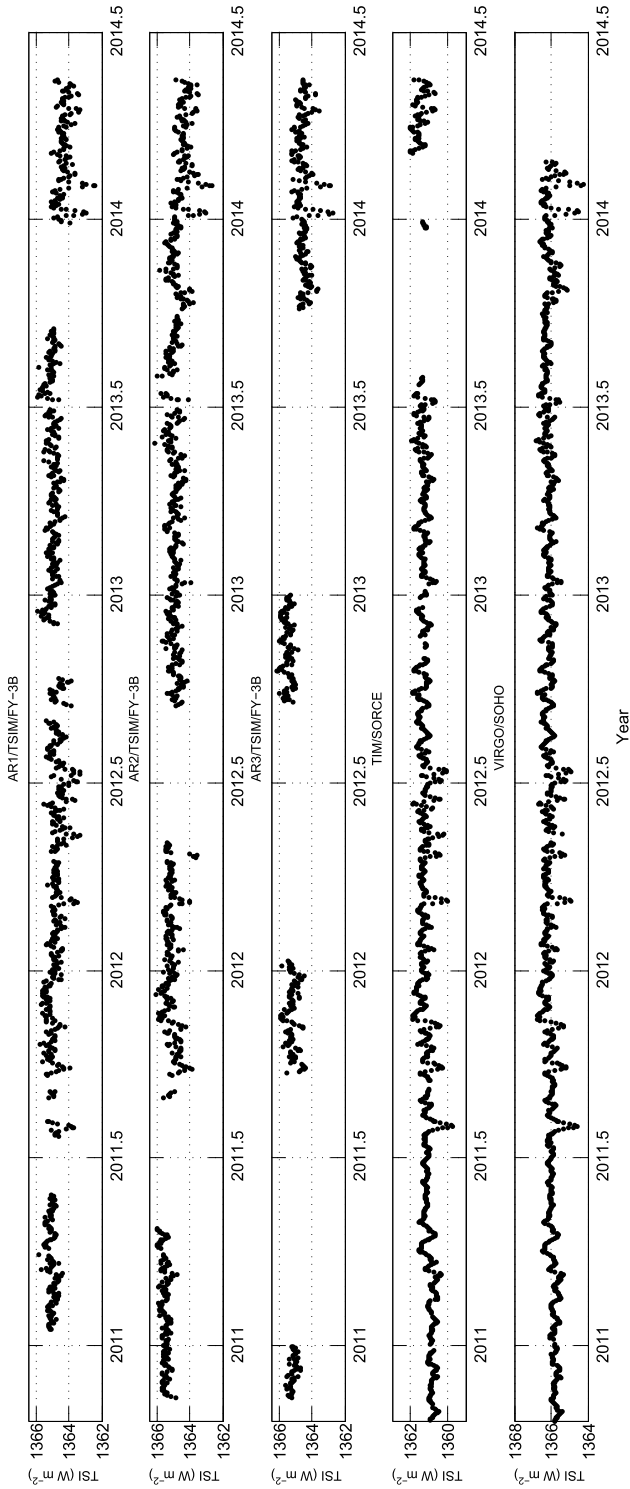


Figure 2 TSI measurements with TSIM/FY-3B (AR1, AR2, and AR3) and TIMSORCE from November 2010 to May 2014. VIRGO/SOHO data are from November 2010 to February 2014. All TSI data are daily averages.

As shown in Figures 2 and 3, the TSI variations detected by TSIM/FY-3B generally agree with TIM/SORCE and VIRGO/SOHO for shorter time scales, while the long-term trend in the TSIM is different from the others. The TSI values of TSIM/FY-3B are generally lower than those from VIRGO/SOHO and slightly higher than those from TIM/SORCE. The offsets between TSIM/FY-3B and the other two space TSI instruments are clear in Figure 3. The offset of about 4 W m^{-2} compared with TIM/SORCE is mainly attributed to different optical layouts of the two instruments (Kopp and Lean, 2011). The aperture arrangement of the instrument plays an important role in this respect (Booth, 2014; Girshovitz and Shaked, 2014). For TIM/SORCE, the precision aperture is located in front of the view-limiting aperture and baffles. The special optical layout of TIM/SORCE was adopted to secure more accurate TSI measurements by eliminating stray light, diffraction effect, and so on. Since TSIM/FY-3B has nearly the same aperture arrangement as VIRGO/SOHO, they show similar values of TSI measurements.

Fehlmann *et al.* (2012) has found that the WRR scale is offset by $\approx 0.3 \%$ with respect to SI. This finding is confirmed by the TSI value offset of TSIM/FY-3B, about 4 W m^{-2} compared with TIM/SORCE.

The FY-3B satellite changed its attitude in September 2013, and sunlight did not enter AR1 for nearly three months. In this period, the shutter of AR1 was always open to detect whether the incoming sunlight was strong enough to return to the solar mode. The sunlight was again received by AR1 on 20 December 2013, but the transition process was quite slow; it took nearly 10 days for the solar pointing error to be smaller than 3° . The incoming sunlight moved slowly to the direction parallel to the optical axis of AR1.

After the FY-3B satellite changed its attitude in September 2013, unexpected improvement in TSI measurements was seen on AR3, and its data quality has become quite good since then. The TSI measurements of AR1, AR2, and AR3 nearly coincide from December 2013 to May 2014, as shown in Figure 1. It shows that now TSIM/FY-3B is in an excellent state of solar observation.

7. Summary and Prospects

The TSI has been measured for nearly four years with TSIM/FY-3B. For most of the time, the short time-scale variations of the TSI recorded by TSIM/FY-3B agree well with VIRGO/SOHO and TIM/SORCE. However, TSIM/FY-3B shows somewhat larger noise and a long-term trend different from the other two instruments. Its larger noise is mainly attributed to the solar pointing errors. Some TSI measurements had to be discarded due to abnormal solar pointing errors computed based on astronomical ephemeris. The scanning observations of TSIM/FY-3B have led to complex estimation problems of the solar pointing errors. This problem was solved by the new instrument TSIM/FY-3C, which has a pointing system. Nevertheless, the passive scanning observations have some advantages; since it requires no complex pointing system for solar tracking, it is an economical solution to a tight budget and it is much more reliable for long-time space flights. Satellite-Sun distance correction for TSI data of TSIM/FY-3B will be performed in the future. In addition, TSIM/FY-3B has reached its three-year design lifetime, but it is still in good health.

It would be beneficial if TSI instrument groups can establish common standards and methods for TSI calibration and data reduction. We hope that the instrument drift seen in our data may be removed by introducing such standard procedures. It is important that the TSI data from various space solar radiometers are compared using the same data calibration and reduction procedures.

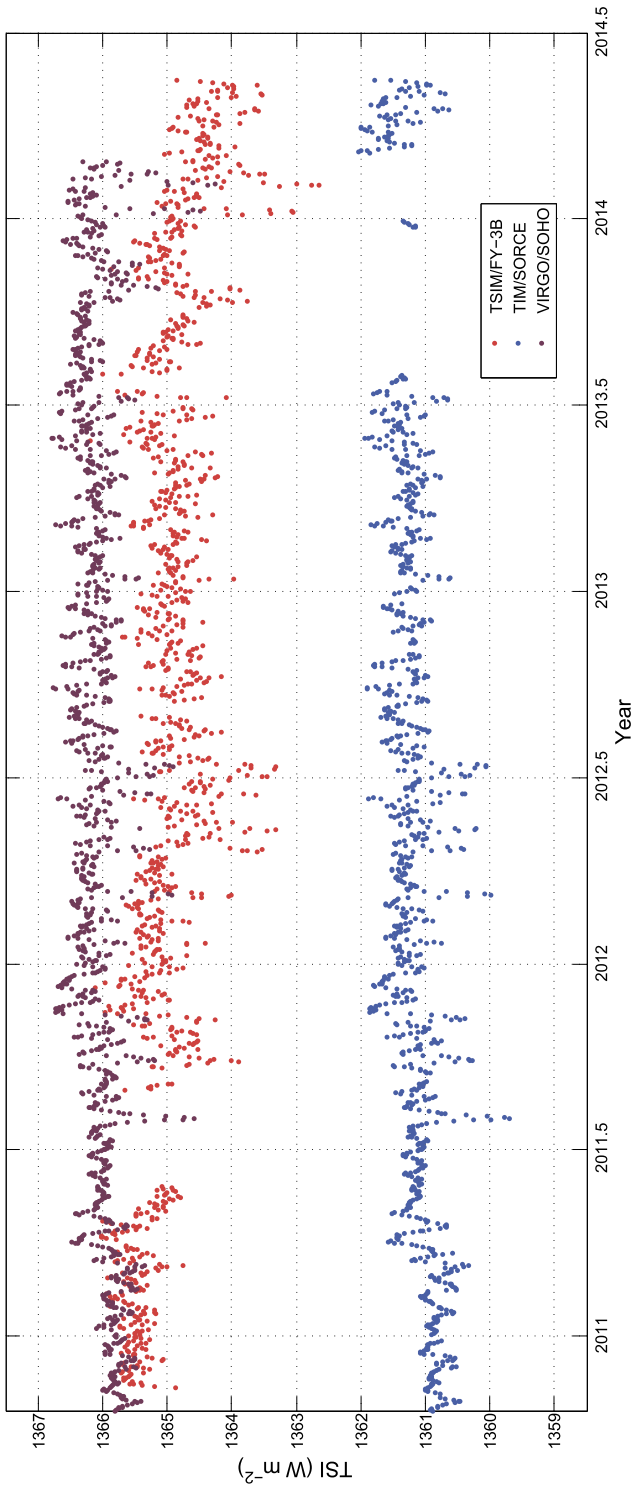


Figure 3 TSI data of TSM/FY-3B composite (red) combining AR1, AR2, and AR3, and TIM/SORCE data (blue) from November 2010 to May 2014. VIRGO/SOHO data (purple) are from November 2010 to February 2014. All TSI data are daily averages.

Acknowledgements This work is supported by the Development Plan Project for Science and Technology of Jilin Province (No. 20130101044JC), Basic Research Project for application of Yunnan Province (No. 2012FD050) and Natural Science Foundation of China (No. 61077080). The authors would like to thank the many people engaged in the TSIM project for their hard work and technical support, including Chenghu Gong, Baoqi Song, Xin Ye in Changchun Institute of Optics, Fine Mechanics and Physic. The authors are grateful to Bingxi Yu, our previous project leader of TSIM, for his great contributions to the TSIM project. The authors would also like to thank for the valuable suggestions and help from the referee. The TSI dataset of TIM/SORCE was generously provided by the TIM team, Laboratory for Atmospheric and Space Physics, University of Colorado, USA. The TSI data of TIM/SORCE were obtained from its web site at <http://lasp.colorado.edu/home/sorce/data/tsi-data/>. The unpublished TSI data of VIRGO/SOHO were provided kindly by the VIRGO team through its FTP site at PMOD/WRC, Davos, Switzerland.

References

- Anklin, M., Frohlich, C., Finsterle, W., Crommelynck, D.A., Dewitte, S.: 1998, Assessment of degradation of VIRGO radiometers on board SOHO. *Metrologia* **35**, 685. DOI.
- Booth, M.: 2014, Adaptive optical microscopy – The ongoing quest for a perfect image. *Light Sci. Appl.* **3**, e165. DOI.
- Bretagnon, P., Francou, G.: 1988, Planetary theories in rectangular and spherical variables – VSOP-87 solutions. *Astron. Astrophys.* **202**, 309.
- Fang, W., Wang, H., Li, H., Wang, Y.: 2014, Total solar irradiance monitor for FY-3A and FY-3B satellites – Instrument design. *Solar Phys.* DOI.
- Fehlmann, A., Kopp, G., Schmutz, W., Winkler, R., Finsterle, W., Fox, N.: 2012, Fourth World Radiometric Reference to SI radiometric scale comparison and implications for on-orbit measurements of the total solar irradiance. *Metrologia* **49**, S34. DOI.
- Frohlich, C.: 2003, Long-term behaviour of space radiometers. *Metrologia* **40**, S60. DOI.
- Frohlich, C.: 2009, Evidence of a long-term trend in total solar irradiance. *Astron. Astrophys.* **501**, L27. DOI.
- Frohlich, C.: 2012, Total solar irradiance observations. *Surv. Geophys.* **33**, 453. DOI.
- Frohlich, C.: 2013, Total solar irradiance: What have we learned from the last three cycles and the recent minimum? *Space Sci. Rev.* **176**, 237. DOI.
- Frohlich, C., Romero, J., Roth, H., Wehrli, C., Andersen, B.N., Appourchaux, T., Domingo, V., Telljohann, U., Berthomieu, G., Delache, P., Provost, J., Toutain, T., Crommelynck, D.A., Chevalier, A., Fichot, A., Däppen, W., Gough, D., Hoeksema, T., Jiménez, A., Gómez, M.F., Herreros, J.M., Cortés, T.R., Jones, A.R., Pap, J.M., Willson, R.C.: 1995, VIRGO: Experiment for helioseismology and solar irradiance monitoring. *Solar Phys.* **162**, 101. DOI.
- Frohlich, C., Andersen, B.N., Appourchaux, T., Berthomieu, G., Crommelynck, D.A., Domingo, V., Fichot, A., Finsterle, W., Gomez, M.F., Gough, D., Jimenez, A., Leifsen, T., Lombaerts, M., Pap, J.M., Provost, J., Cortes, T.R., Romero, J., Roth, H., Sekii, T., Telljohann, U., Toutain, T., Wehrli, C.: 1997a, First results from VIRGO, the experiment for helioseismology and solar irradiance monitoring on SOHO. *Solar Phys.* **170**, 1. DOI.
- Frohlich, C., Crommelynck, D.A., Wehrli, C., Anklin, M., Dewitte, S., Fichot, A., Finsterle, W., Jiménez, A., Chevalier, A., Roth, H.: 1997b, In-flight performance of the VIRGO solar irradiance instruments on SOHO. *Solar Phys.* **175**, 267. DOI.
- Girshovitz, P., Shaked, N.: 2014, Doubling the field of view in off-axis low-coherence interferometric imaging. *Light Sci. Appl.* **3**, e151. DOI.
- Kopp, G., Heuerman, K., Lawrence, G.: 2005, The total irradiance monitor (TIM): Instrument calibration. *Solar Phys.* **230**, 111. DOI.
- Kopp, G., Lawrence, G.: 2005, The total irradiance monitor (TIM): Instrument design. *Solar Phys.* **230**, 91. DOI.
- Kopp, G., Lawrence, G., Rottman, G.: 2005, The total irradiance monitor (TIM): Science results. *Solar Phys.* **230**, 129. DOI.
- Kopp, G., Lean, J.L.: 2011, A new, lower value of total solar irradiance: Evidence and climate significance. *Geophys. Res. Lett.* **38**, L01706. DOI.
- Kopp, G., Fehlmann, A., Finsterle, W., Harber, D., Heuerman, K., Willson, R.: 2012, Total solar irradiance data record accuracy and consistency improvements. *Metrologia* **49**, S29. DOI.
- Liebetraut, P., Petsch, S., Liebeskind, J., Zappe, H.: 2013, Elastomeric lenses with tunable astigmatism. *Light Sci. Appl.* **2**, e98. DOI.
- Meftah, M., Dewitte, S., Irbah, A., Chevalier, A., Conscience, C., Crommelynck, D., Janssen, E., Mekaoui, S.: 2014, SOVAP/Picard, a spaceborne radiometer to measure the total solar irradiance. *Solar Phys.* **289**, 1885. DOI.

- Mekaoui, S., Dewitte, S., Conscience, C., Chevalier, A.: 2010, Total solar irradiance absolute level from DIARAD/SOVIM on the international space station. *Adv. Space Res.* **45**, 1393. [DOI](#).
- Memarian, M., Eleftheriades, G.: 2013, Light concentration using hetero-junctions of anisotropic low permittivity metamaterials. *Light Sci. Appl.* **2**, e114. [DOI](#).
- Rubenchik, A., Fedoruk, M., Turitsyn, S.: 2014, The effect of self-focusing on laser space-debris cleaning. *Light Sci. Appl.* **3**, e159. [DOI](#).
- Wang, H., Li, H., Fang, W.: 2014, Timing parameter optimization for comparison experiments of TSIM. *Appl. Opt.* **53**, 1718. [DOI](#).
- Witte, S., Tenner, V., Noom, D., Eikema, K.: 2014, Lensless diffractive imaging with ultra-broadband tabletop sources: From infrared to extreme-ultraviolet wavelengths. *Light Sci. Appl.* **3**, e163. [DOI](#).
- Yang, Z., Lu, N., Shi, J., Zhang, P., Dong, C., Yang, J.: 2012, Overview of FY-3 payload and ground application system. *IEEE Trans. Geosci. Remote Sens.* **50**, 4846. [DOI](#).